Proc. Natl. Acad. Sci. USA
Vol. 89, pp. 11547–11551, December 1992
Biophysics

Morphological changes in liposomes caused by polymerization of encapsulated actin and spontaneous formation of actin bundles

(cytoskeleton)

HIDETAKE MIYATA*† AND HIROKAZU HOTANI‡

*Department of Physics, Faculty of Science and Technology, Keio University, 3-14-1 Hiyoshi, Kohoku-ku, Yokohama 223, Japan; and ‡Department of Biosciences, Teikyo University, Toyosatodai, Utsunomiya 320, Japan

Communicated by Marc Kirschner, July 16, 1992

ABSTRACT **Spherical giant liposomes that had encapsulated skeletal-muscle G-actin were made by swelling a dried lipid mixture of dimyristoyl phosphatidylcholine/cardiolipin, 1:1 (wt/wt), in a solution of G-actin/$CaCl_2$ at 0°C. Polymerization of the encapsulated G-actin into actin filaments was achieved by raising the temperature to 30°C. We observed the subsequent shape changes of the liposomes by dark-field and differential interference-contrast light microscopy. After ≈40 min, which was required for completion of actin polymerization, two shapes of liposome were evident: dumbbell and disk. Elongation of the dumbbell-shaped liposomes was concomitant with actin polymerization. Polarization microscopy showed that actin filaments formed thick bundles in the liposomes and that these filaments lay contiguous to the periphery of the liposome. Localization of actin filaments in the liposomes was confirmed by observation of rhodamine phalloidin-conjugated actin filaments by fluorescence microscopy. Both dumbbell- and disk-shaped liposomes were rigid and kept their shapes as far as actin filaments were stabilized. In contrast, liposomes containing bovine serum albumin were fragile, and their shapes continually fluctuated from Brownian motion, indicating that the actin bundles served as mechanical support for the liposome shapes.**

F-actin, the filamentous polymer of globular G-actin, is involved in a variety of cellular functions, such as extension of microspikes from tissue culture cells (1), contraction of the contractile ring during cell division (2), and extension or retraction of pseudopods in amoeboid movement (3). Actin filaments also serve as mechanical support in structures; these include stress fibers in various cells (4), microvilli of intestinal brush border cells (5, 6), and stereocilia of hair cells in the inner ear (7). In these structures, F-actin forms bundles or networks to achieve sufficient mechanical stiffness.

Microtubules are considered another cytoskeletal element that functions to develop and maintain cell shape. Miyamoto and Hotani (8) have made liposomes that encapsulated tubulin, the subunit protein of microtubules. Liposomes are closed vesicles of lipid-bilayer membrane, and their characteristics have been well-studied as models of biological membranes. Miyamoto and Hotani have also shown that the tubulin polymerization in liposomes forms membrane projections from the liposome surface. Extension of these projections is from the growth of microtubules by tubulin assembly, indicating that microtubules possess sufficient intrinsic stiffness to deform the membrane.

In another study, G-actin was encapsulated in liposomes by the diethyl ether-injection method, and then the actin was polymerized by the valinomycin-mediated introduction of K^+ ions (9). The authors showed that actin did polymerize, and they obtained irregularly shaped liposomes that were observed by light microscopy. However, the relation between actin polymerization and liposome deformation has remained unclear.

To study the possible role of F-actin in the morphogenesis of biological cells, we developed a method to incorporate G-actin into liposomes and then to polymerize the actin by modifying the method of tubulin polymerization in liposomes (8). We monitored the dynamic transformation processes of the liposomes resulting from actin polymerization by dark-field and differential interference-contrast (DIC) light microscopy and found that the initially spherical liposomes changed to one of two regular shapes having geometrical symmetry: dumbbell or disk shape. We also found that when G-actin polymerized into filaments in a liposome, the filaments spontaneously aligned along the periphery of the liposome to form bundles.

MATERIALS AND METHODS

Actin. Actin was prepared from rabbit skeletal muscle by the method of Spudich and Watt (10) and was further purified by gel filtration with Sephadex G-150 (Pharmacia).

Preparation of Liposomes. Seventy micrograms of dimyristoyl phosphatidylcholine was dissolved in a chloroform/methanol mixture, 98:2 (vol/vol), and 70 μg of cardiolipin in chloroform was added. The organic solvent was then evaporated under a flow of nitrogen gas. The lipids were further dried *in vacuo* for at least 2 hr and stored at −20°C.

To prepare liposomes encapsulating actin, 25 μl of a 100 μM solution of G-actin in buffer A (2 mM Tris·HCl, pH 8.2/0.5 mM $CaCl_2$/0.2 mM ATP/0.2 mM NaN_3/0.5 mM dithiothreitol) was added to the dried lipid film. For the control experiment, liposomes containing bovine serum albumin (BSA) were made by the same method. Upon liquid addition, the lipid film immediately started swelling to form liposomes. Swelling was facilitated by agitating the test tube occasionally by hand. After 1 hr, to prevent polymerization of actin outside the liposomes, the liposome suspension was diluted 50-fold with 100 μM BSA in buffer A. All procedures were done on ice.

Polymerization of Actin in Liposomes. Polymerization of G-actin in liposomes was initiated by raising the temperature from 10°C to 30°C. To prevent polymerization before starting observation, the glass slide and coverslip were placed on a precooled aluminum block. Three microliters of diluted liposome suspension was placed on the slide, the cover glass (22 × 22 mm) was placed on the sample, and it was sealed with silicone grease to prevent evaporation of the solvent. Temperature of the microscope specimen could be kept <10°C by this procedure. Warm air was gently blown over the specimen to raise the temperature, initiating the polymerization of G-actin in the liposomes. The flow of warm air

The publication costs of this article were defrayed in part by page charge payment. This article must therefore be hereby marked "*advertisement*" in accordance with 18 U.S.C. §1734 solely to indicate this fact.

Abbreviations: DIC, differential interference contrast; BSA, bovine serum albumin.

†To whom reprint requests should be addressed.

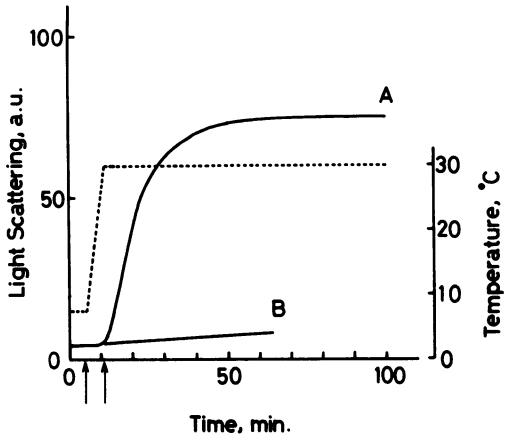

FIG. 1. Light scattering measured at 400 nm (—) to follow actin polymerization initiated by raising temperature. Initially G-actin (100 μM) in 2 mM Tris·HCl, pH 8.2/0.5 mM $CaCl_2$/0.2 mM ATP/0.2 mM NaN_3/0.5 mM dithiothreitol was incubated in a cuvette at 8°C; then the temperature was raised to 30°C during the time between the two arrows (curve A) or kept at 8°C (curve B). ---, Time course of change in temperature of actin solution.

was continued during the microscopic observation to maintain the temperature of the sample at ≈30°C.

Light Scattering Measurement. Actin polymerization was followed by monitoring light scattering at 400 nm with a spectrofluorophotometer (model 650-10S, Hitachi).

Visualization of F-Actin in Liposomes. A 3.3 μM solution of rhodamine-conjugated phalloidin in methanol was mixed with the lipid solution and then dried to prepare lipid films used for making liposomes. The rhodamine-conjugated phalloidin specifically bound to F-actin, so that actin bundles became visible under a fluorescence microscope (11).

Microscopic Observation and Video Recording. A dark-field microscope (model BHF, Olympus) using a 200 W high-pressure mercury lamp as a light source and a microscope (Optiphot, Nikon) equipped with DIC or polarization optics were used to observe liposomes.

The images obtained by dark-field microscopy were recorded with a silicon-intensified target camera (model C 2400, Hamamatsu Photonics). The images obtained with DIC or polarization microscopy were recorded with a video camera (model WV 1550, Panasonic). These images were further processed with an image processor (Image Sigma, Avionics) to enhance contrast.

RESULTS

Formation of Liposomes Encapsulating Actin. To study the role of actin filaments in vesicular morphogenesis, the following two steps must be controlled separately: (*i*) formation of liposomes containing G-actin and (*ii*) shape change of the liposome caused by actin polymerization. We have searched for the best combination of lipids for making liposomes at 0°C in buffer A, as polymerization of G-actin can be suppressed completely at this temperature (Fig. 1). The lipid mixture of cardiolipin/dimyristoyl phosphatidylcholine, 1:1 (wt/wt) was found most suitable for forming liposomes at 0°C, which is much lower than the phase-transition temperature of dimyristoyl phosphatidylcholine alone (≈23°C). Fig. 1 shows that actin polymerization was suppressed almost completely at 8°C, whereas polymerization started when the temperature was raised to 30°C.

A previous study (12) demonstrated that actin binding to the lipid-bilayer membrane could be suppressed when the membrane was made from a mixture of neutral and negatively charged lipids.

Immediately after preparation of the actin-containing liposomes, their shapes were usually spherical. These spherical liposomes, however, transformed into either dumbbell or disk shapes (which were geometrically symmetrical) when the encapsulated actin was polymerized by raising the temperature (see Figs. 3 and 4).

Different views of a floating liposome clearly show that the expanded portion at the end of the dumbbell shape is flat, not spherical. The disk-shaped liposomes were formed more frequently than dumbbell-shaped liposomes. Sometimes, the number of disk-shaped liposomes was >10 times that of the dumbbell-shaped ones. When Ca^{2+} was eliminated from the liposome suspension, suppressing actin polymerization, neither disk- nor dumbbell-shaped liposomes were ever formed.

Morphological Change of a Dumbbell-Shaped Liposome. We monitored the morphological change of a dumbbell-shaped liposome by dark-field microscopy (Fig. 2). One can readily see an increase in length and decrease in width of the connecting-bar portion of the dumbbell shape. The elongation continued for 45 min and then stopped; further observation for 60 min showed no significant shape change.

There was a bright spot in each disk portion of the dumbbell-shaped liposomes. The disk portions are slightly concave. This curvature change might cause anomalously strong light scattering in dark-field microscopy.

The dumbbell-shaped liposomes have a fairly rigid structure, as judged by the low-level fluctuation in their shapes. Their membranes were quiescent, and bending motions were restrained. On the other hand, the BSA-containing liposomes displayed an undulating circumference and did not assume any definite shape (Fig. 3 *d–f*).

F-Actin Arrangement in a Dumbbell-Shaped Liposome. Because liposomes containing actin were more rigid than those containing BSA, we thought some stable structure might be formed when actin polymerized. The most probable structure is a bundle of F-actin. If there were a bundle in a liposome, it should provide birefringence and become visible by polarization microscopy.

Fig. 3 *a* and *b* shows polarization micrographs of a dumbbell-shaped liposome. The longitudinal axis of the liposome was set at a 45° angle clockwise from the axis of the polarizer in *a*; the longitudinal axis was set at a 45° angle counterclockwise in *b*. These figures clearly show the existence of birefringence along the liposome contour. This birefringent zone occupied all of the bar portion and branched into two

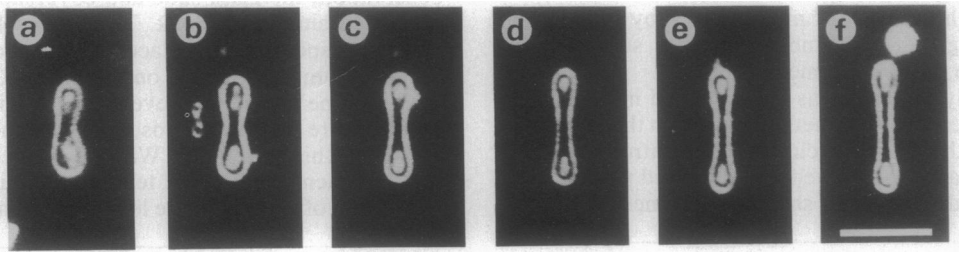

FIG. 2. Process of deformation of a liposome containing actin. Dark-field micrographs were taken at 5 min (*a*), 7 min (*b*), 10 min (*c*), 15 min (*d*), 30 min (*e*), and 45 min (*f*) after actin polymerization was initiated by raising temperature. (Bar = 10 μm.)

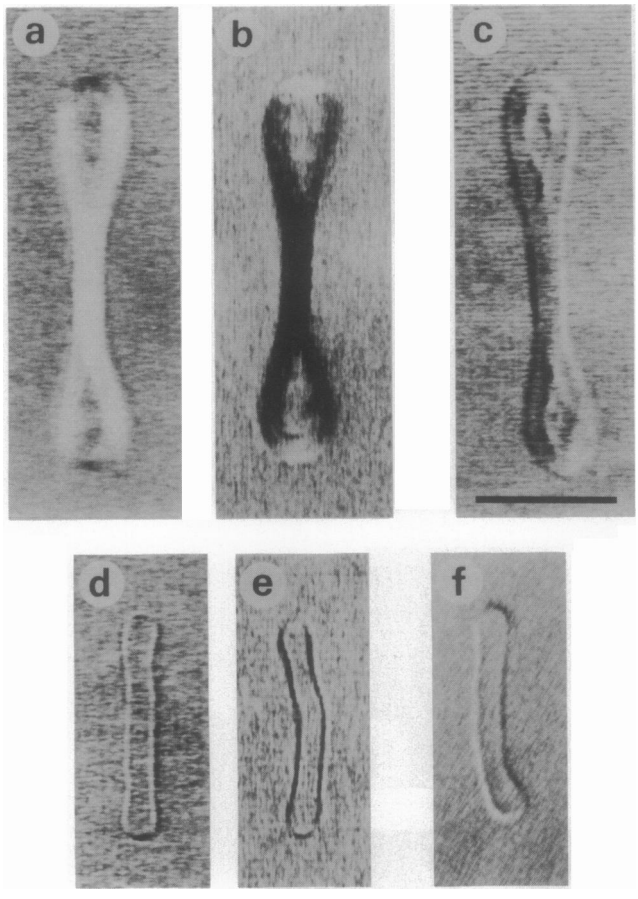

FIG. 3. Actin bundles in a dumbbell-shaped liposome. (*a* and *b*) Polarization micrographs of a dumbbell-shaped liposome containing actin. Images were taken with the longitudinal axis of the liposome set clockwise (*a*) and counterclockwise (*b*) at a 45° angle with respect to the polarizer axis. (*c*) DIC micrograph of the same liposome as in *a* and *b*. (*d* and *e*) Polarization micrograph of BSA-containing liposome. Longitudinal axes of the liposome in *d* and *e* were set clockwise and counterclockwise at a 45° angle from the polarizer axis, respectively. (*f*) DIC micrograph of the same liposome. (Bar = 10 μm.)

zones at each disk portion. No birefringence occurred in the center of either disk portion. This birefringence must result from the formation of bundles of aligned F-actin filaments because the liposomes containing BSA did not give any birefringence except that arising from the lipid-bilayer membrane (Fig. 3 *d* and *e*).

To determine the relationship between birefringence and orientation of the F-actin, we examined the birefringent image of a paracrystal of F-actin in which the alignment of F-actin was well established. The paracrystals were developed in 10 mM $MgCl_2$. The result showed that the longitudinal axis of F-actin paralleled the longitudinal direction of the birefringent zone, where a bundle of F-actins existed.

There was a domain lacking birefringence in each disk portion of the dumbbell-shaped liposome. Polarization microscopy alone is not able to determine whether this lack was caused from random orientation of F-actin or from a low concentration of F-actin. A DIC micrograph (Fig. 3*c*) of this liposome shows strong contrast along the periphery of this domain, indicating substantial difference in actin concentrations between birefringent and nonbirefringent domains; there was much less actin in the central domain of the disk portion. This result was confirmed by the visualization of encapsulated F-actin by fluorescence microscopy (see Fig. 6).

Alignment of F-Actin in a Disk-Shaped Liposome. Alignment of F-actin filaments in a disk-shaped liposome was

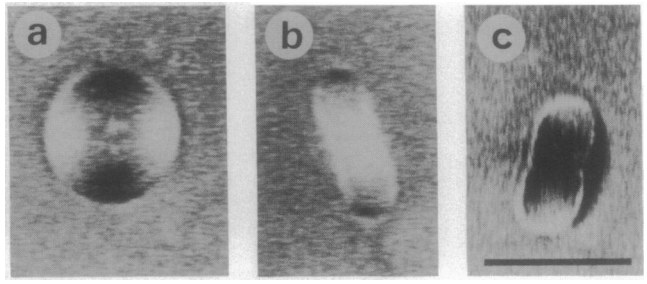

FIG. 4. Polarization micrograph of disk-shaped liposome containing actin. (*a*) Front view. (*b* and *c*) Side views. The polarizer was set 45° clockwise (*b*) or counterclockwise (*c*) off vertical. (Bar = 10 μm.)

examined similarly. Fig. 4 *a–c* shows birefringence patterns of a disk-shaped liposome. In the front view (*a*), the birefringent zone was localized along the periphery, as observed with the dumbbell-shaped liposome. The birefringence appeared as two dark and two bright sectors, which were alternately aligned to form a circle. The position of dark and bright sectors did not move when the microscope stage was rotated, indicating that F-actin formed bundles that were laid circularly around the liposome center. Birefringence patterns in the side views (*b* and *c*) were obtained by setting the longitudinal axis of the image at a 45° angle clockwise or counterclockwise to the polarizer axis. These patterns confirm alignment of the bundle described above: the actin bundle runs parallel to the longitudinal axis of the side view.

Shape Change of a Disk-Shaped Liposome Accompanied by Actin Polymerization. Fig. 5 *Upper* demonstrates the development of birefringence in a disk-shaped liposome. Birefringence was almost negligible until 6 min (*c*), but it became recognizable at 16 min (*d*). Twenty-four minutes later (*e*) birefringence became more prominent, and an additional change—extinction of birefringence from the central part—began; the latter change continued up to 73 min (*g*); then no further appreciable change occurred (data not shown). Concomitant with these changes, thickness of the liposome decreased, as shown in the side views (Fig. 5 *Lower*). At the beginning, the liposome was spherical (*a'*). However, it started to dimple at 16 min (*d'*), and the dimple became so deep that the two opposite lipid bilayers almost contacted each other at 24 min (*e'*). Finally, the liposome was almost completely compressed (*f'*) and lost its thickness except in the narrow peripheral zone where actin bundles formed a circle.

Because this liposome kept symmetrical geometry during the transformation, we could easily determine its total surface area from the shapes of front and side views; the total surface area remained constant during the shape change.

Visualization of F-Actin in Liposomes Using Rhodamine-Conjugated Phalloidin. Localization of F-actin in the semi-dumbbell-shaped and disk-shaped liposomes is shown in Fig. 6 *a* and *b*. Two domains are evident in those liposomes: one with and another without F-actin, as indicated by the distribution of rhodamine fluorescence. By comparing these images with polarization micrographs (Figs. 3 and 4), F-actin was clearly absent from the areas that lacked birefringence. This uneven distribution of rhodamine fluorescence was not caused from interaction of rhodamine-conjugated phalloidin molecules with the membrane because the rhodamine fluorescence was uniformly distributed in the liposomes containing BSA (Fig. 6*c*).

DISCUSSION

We have described the characteristic morphologies of liposomes in which stable shape was acquired as a result of actin

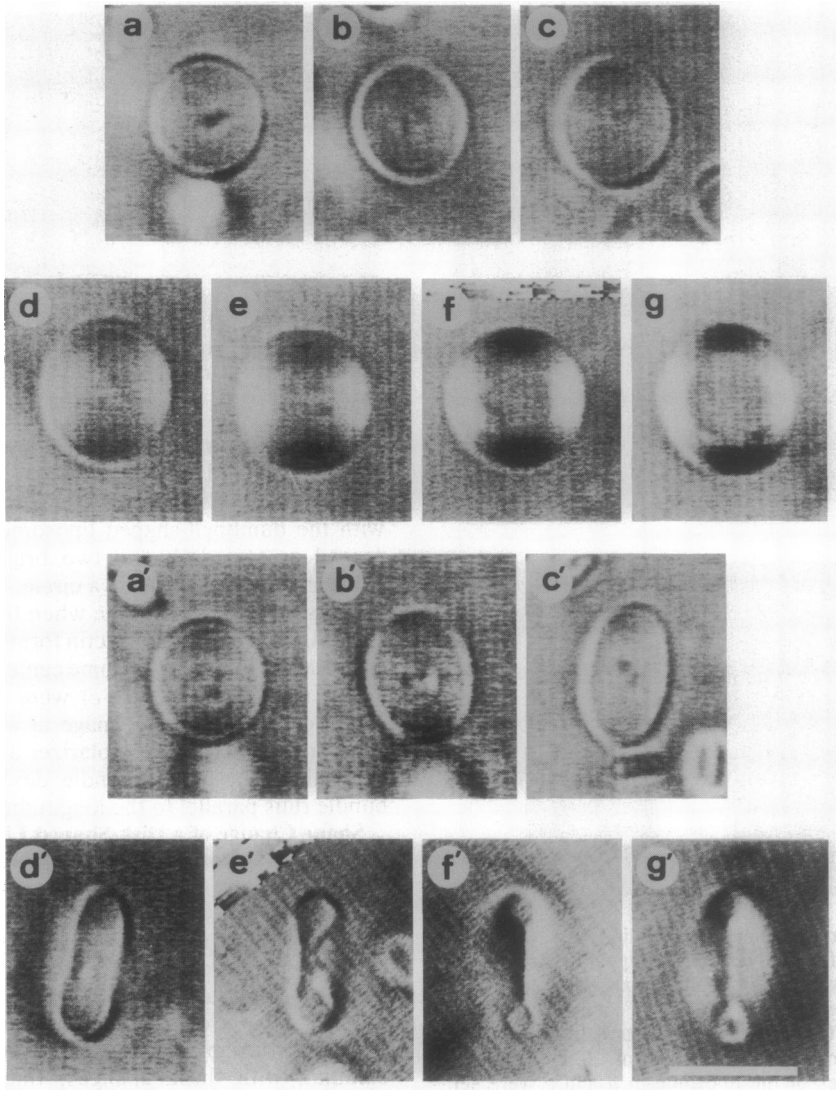

FIG. 5. Birefringence development of disk-shaped liposome. (*a–g*) Series of front views: 0 min (*a*), 1 min (*b*), 6 min (*c*), 16 min (*d*), 24 min (*e*), 33 min (*f*), and 73 min (*g*) after start of polymerization. (*a'–g'*) Side views obtained at approximately same time points as those of *a–g*.

polymerization in the liposomes. In contrast, normal liposomes containing no actin are known to transform into various shapes; these transformations are driven by the osmotic-pressure difference between the outside and inside of the liposome (13). The liposomes developed by actin polymerization, however, differ markedly in shape and rigidity from those undergoing changes driven by osmotic-pressure differences. The latter never adopted the dumbbell shape and never possessed a rigid structure, their shapes always fluctuating. In contrast, the actin-containing liposomes formed characteristic shapes and were rigid enough to maintain their morphology. Therefore, the osmotic-pressure difference could not be the primary driving force for transforming the actin-containing liposomes. This interpretation was also confirmed by the fact that the transformation driven by osmotic pressure occurred within several seconds, but that driven by actin polymerization took several tens of minutes.

How actin filaments align contiguous to liposome periphery and assemble into a thick bundle is not yet clear. Self-organization of actin bundles caused by linear shear (14) or osmoelastic stress (15) has been reported. These mecha-

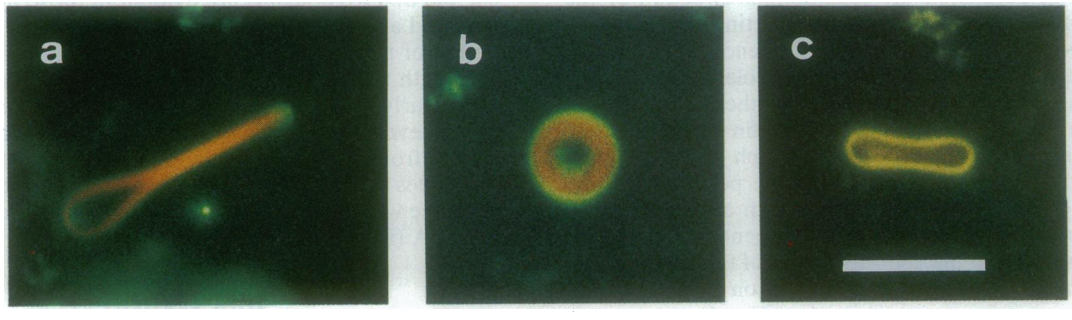

FIG. 6. Visualization of F-actin by fluorescence microscopy. F-actin in semi-dumbbell-shaped (*a*) and disk-shaped (*b*) liposomes was visualized with rhodamine-conjugated phalloidin. (*c*) Liposome containing BSA and rhodamine-conjugated phalloidin. (Bar = 10 μm.)

nisms, however, seem not to be significant in bundle formation in the present case.

Another possible mechanism is that generally thought applicable to explain lateral alignment of rod-like particles (e.g., tobacco mosaic virus) when particle concentration exceeds a critical value (16, 17). In fact, we found that actin solutions at higher concentrations became birefringent upon actin polymerization, indicating that spontaneous alignment of actin filaments occurred without liposomes (unpublished work). However, this alignment occurred on a much larger scale than that with liposomes; the size of the birefringent area was ≈10–20 μm wide and 100 μm long, whereas the size of the liposomes was only up to 10–20 μm in width and length in most cases. In addition, we observed no tendency of the aligned filaments in solution to form circular structures. We thus suggest that restriction of actin filaments within a small space played the major role in the spontaneous formation of circular bundles, as follows.

Before the encapsulated actin polymerized, our liposomes were flaccid, and some parts of the liposomes had less curvature than other parts. When actin filaments grew, they would be unavoidably bent to remain inside the liposome. Once a filament lies along some portion with less curvature, filaments forming subsequently probably align themselves parallel to the preexisting filament to minimize their bending energy. As a result, most filaments align in the same way—that is, they form a bundle in the liposome. This qualitative explanation obviously needs evaluation by future studies.

In an experiment of Cortese *et al.* (9) liposomes changed their shapes from spherical to irregular, and heterogeneous distribution of actin filaments was seen when encapsulated actin was polymerized. These workers ascribed this result to discrete nucleation sites for polymerization: filaments grown from these sites acted as primers for forming a few larger filament bundles—hence, these filaments led to heterogeneous actin distribution. In our system liposome shape and actin distribution were more regular after polymerization was completed. We believe the difference was from the agent used to initiate actin polymerization: K^+ ions were used in Cortese's system, whereas we used Ca^{2+} ions. K^+ ions have been shown to promote actin nucleation, but Ca^{2+} suppresses the process, and polymerization itself is slower (18). We assume that in Cortese's system nucleation was immediately followed by primer formation and subsequent filament elongation, so that rearrangement of actin filaments via diffusion became difficult because of the short time during which filaments could diffuse before polymerization was complete. Hence, filament distribution would have been strongly influenced by the initial distribution of nuclei, which was probably uneven. In our system, on the other hand, the slower nucleation and elongation process probably allowed actin filaments to rearrange for a longer time, which allowed a more regular filament distribution. A more recent report (19) shows that actin polymerization in liposomes from introducing K^+ or Mg^{2+} ions with ionophores caused the liposome shape to change from an elongated form to an oblate ellipsoid.

The morphological difference between liposomes containing actin and tubulin (8) must originate from the difference in rigidities between an actin filament and a microtubule (20, 21). A few microtubules were presumably strong enough to make membrane protrusions. On the other hand, actin filaments would be unable to make such a protrusion unless clustered with the aid of the actin-bundling proteins to gain sufficient mechanical strength (22, 23).

Recent studies (24, 25) strongly indicate the involvement of actin, both in dynamic and static aspects of cellular activities. Rinnerthaler *et al.* (25) were able to correlate leading-edge movement with microfilament structure in the lamellae of single mouse peritoneal macrophage cells. These workers observed actin bundle structures along relatively immobile portions of the lamellar edge.

Our observation that thermal fluctuation of the lipid-bilayer membrane was greatly reduced by the presence of actin bundles, which closely contact the membrane and may serve as a lining, emphasizes a mechanical role for actin bundles in stabilizing cellular membranes.

We thank Dr. Christopher Jones for critical reading of the manuscript and helpful comments. We are also much indebted to Dr. Issei Mabuchi for valuable comments.

1. Albrecht-Buehler, G. & Lancaster, R. M. (1976) *J. Cell Biol.* **71**, 370–382.
2. Schroeder, T. E. (1973) *Proc. Natl. Acad. Sci. USA* **70**, 1688–1692.
3. Taylor, D. L. & Condeelis, J. S. (1979) *Int. Rev. Cytol.* **56**, 57–144.
4. Byers, H. R. & Fujiwara, K. (1982) *J. Cell Biol.* **93**, 804–811.
5. Mukherjee, T. M. & Staehelin, L. A. (1971) *J. Cell Sci.* **8**, 573–599.
6. Tilney, L. G. & Mooseker, M. (1971) *Proc. Natl. Acad. Sci. USA* **68**, 2611–2615.
7. DeRosier, D. J., Tilney, L. G. & Egelman, E. (1980) *Nature (London)* **287**, 291–296.
8. Miyamoto, H. & Hotani, H. (1990) *Adv. Biophys.* **26**, 135–156.
9. Cortese, J. D., Schwab, B., III, Frieden, C. & Elson, E. L. (1989) *Proc. Natl. Acad. Sci. USA* **86**, 5773–5777.
10. Spudich, J. A. & Watt, S. (1971) *J. Biol. Chem.* **246**, 4866–4871.
11. Wieland, T., deVries, J. X., Schafer, A. & Faulstich, H. (1975) *FEBS Lett.* **54**, 73–75.
12. Laliberte, A. & Gicquaud, C. (1988) *J. Cell Biol.* **106**, 1221–1227.
13. Hotani, H. (1984) *J. Mol. Biol.* **178**, 113–120.
14. Cortese, J. D. & Frieden, C. (1988) *J. Cell Biol.* **107**, 1477–1487.
15. Suzuki, A., Yamazaki, M. & Ito, T. (1989) *Biochemistry* **28**, 6513–6518.
16. Onsager, L. (1949) *Ann. N.Y. Acad. Sci.* **52**, 627–659.
17. Oster, G. (1950) *J. Gen. Physiol.* **33**, 445–473.
18. Tobacman, L. S. & Korn, E. D. (1983) *J. Biol. Chem.* **258**, 3207–3214.
19. Bärmann, M., Käs, J., Kurzmeier, H. & Sackmann, E. (1992) in *The Structure and Conformation of Amphiphilic Membranes*, eds. Lipowsky, R., Richter, D. & Kremer, K. (Springer, Heidelberg).
20. Mizushima-Sugano, J., Maeda, T. & Miki-Noumura, T. (1983) *Biochim. Biophys. Acta* **755**, 257–262.
21. Egelman, E. H. (1985) *J. Muscle Res. Cell Motil.* **6**, 129–151.
22. Fechheimer, M. (1987) *J. Cell Biol.* **104**, 1539–1551.
23. Tilney, L. G., Fukui, Y. & DeRosier, D. J. (1987) *J. Cell Biol.* **104**, 981–993.
24. Theriot, J. A. & Mitchison, T. J. (1991) *Nature (London)* **352**, 126–131.
25. Rinnerthaler, G., Herzog, M., Klappacher, M., Kunka, H. & Small, J. V. (1991) *J. Struct. Biol.* **106**, 1–16.